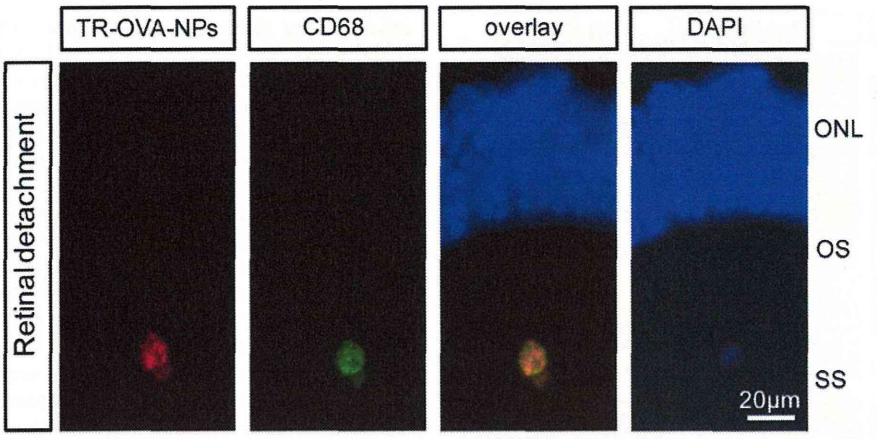

Fig. 8. Accumulation of NPs in the inflamed cells after retinal detachment. In the eye with retinal detachment, TR-OVA-NPs were detected in the recruited monocytes under the sub-retinal space (upper panels) and detected in the recruited CD11b (+) cells in the vitreous cavity. Scale bar = 20 μm. GCL: ganglion cell layer, IPL: inner plexiform layer, ONL: outer nuclear layer, OS: outer segment, and SS: sub-retinal space.

are a potential vehicle for long-term drug delivery in the damaged retina.

The size of the NPs used in this study was approximately 200 nm. This size limits the internalization of NPs to phagocytic cells, as they are too large to diffuse through intact cell membranes. The process of macrophage phagocytosis leads to fragmentation of γ-PGA-Phe by various enzymes (pronase E, protease, cathepsin B, and lipase). In this way, the contents of the NPs are released into the cytosol of the

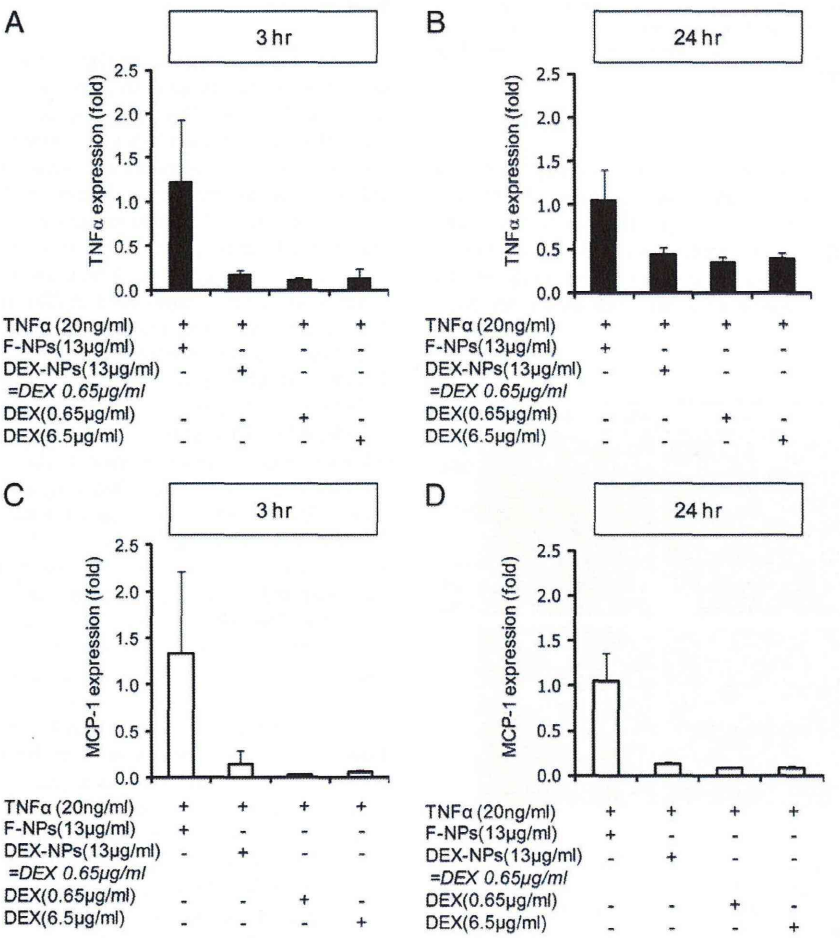

Fig. 9. DEX-NPs suppress the expression of mRNA for TNFα and MCP-1 in the cultured macrophages. The bar charts demonstrate the expressional changes of TNFα and MCP-1 at 3 h (upper panels) and 24 h (lower panels) *in vitro*. Both DEX-NPs and DEX alone had a similar potential for suppressing the activated macrophages.

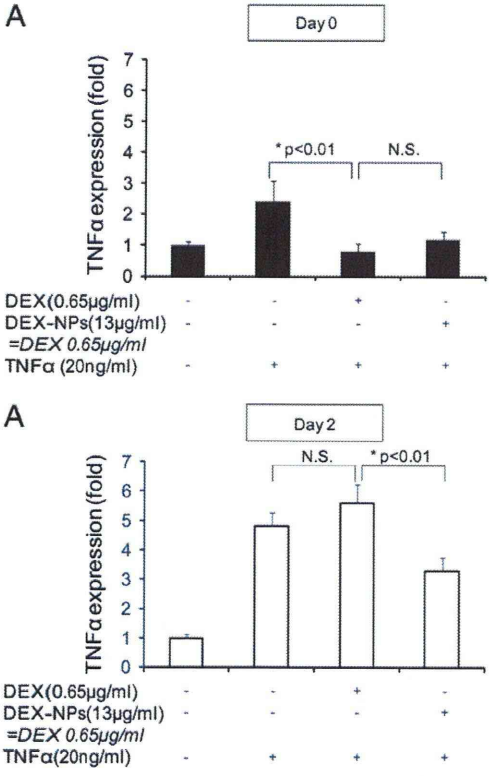

Fig. 10. DEX-NPs had a longer anti-inflammatory effect in the cultured macrophages. The bar charts show the expressional changes of TNFα at 2 h after TNFα stimulation. After 2 h of incubation, DEX-NPs and DEX alone had a similar potential for suppressing TNFα-induced macrophage activation.

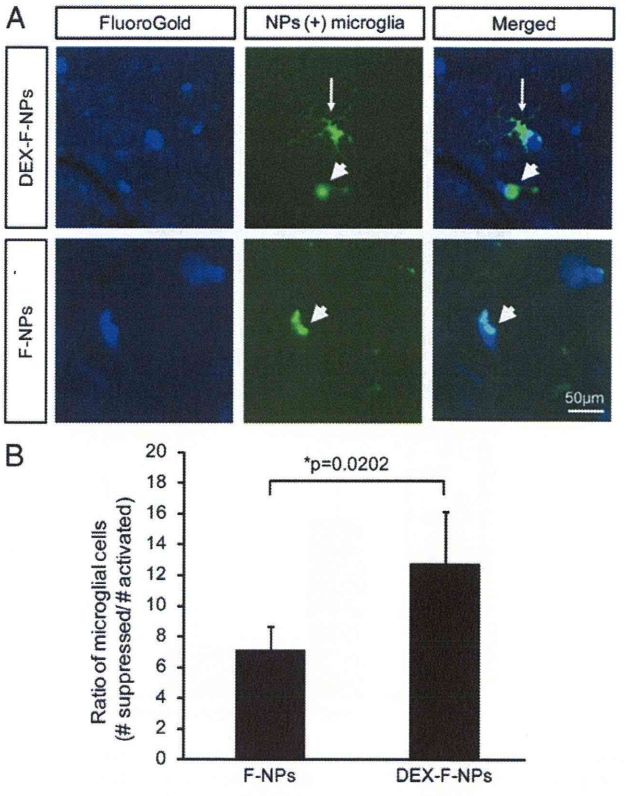

Fig. 11. The effect of DEX-NPs on NMDA-induced microglial activation. A: A representative photograph of the flat-mounted retina 7 days after injury with NMDA. DEX-F-NPs (A: upper panels), but not F-NPs (A: lower panels), suppress the morphological changes in microglia from NMDA-induced retinal damage. The white arrow indicates the resting microglia (ramified shapes) and the arrowheads indicate the activated microglia (amoeboid shapes). B: Quantitative data for the ratio of the numbers of "suppressed microglia" and "activated microglia". Scale bar = 50 μm.

phagocytic cells. Hence, various other molecules are potential candidates to be used with this delivery platform, including ligands for nuclear receptors or modulators of signal transduction, transcription, or translation. In this study, in order to investigate whether released drugs were effective, we chose DEX because it binds to a nuclear receptor. Other possible uses of γ-PGA-Phe NPs could be to deliver small peptides, siRNA, antisense DNA, and various small compounds. The use of PLA and PLGA, other common candidates for drug delivery systems, is limited by the choice of molecules. Thus, γ-PGA-Phe NPs enabled us to specifically target macrophages and microglia using various approaches.

Clinically, steroids are potent drugs to suppress inflammation. Subtenon or intravitreal administration of triamcinolone acetate (IVTA), a type of steroid, has been effective in the treatment of several retinal disorders, including uveitis, diabetic macular edema, laser injury, and branch or central retinal vein occlusion [31,32]. However, 30 to 40% of patients with IVTA experienced complications of steroid-induced glaucoma [33–35] and post-capsular cataract formation [36], and 59% of patients with preexisting glaucoma required additional glaucoma medications [33]. Furthermore, direct administration of steroids is toxic for retinal neurons [37]. Our results suggest that γ-PGA-Phe NPs open a new avenue for minimizing the complications of steroid treatment by specifically targeting macrophages and microglia. These NPs have been applied to several systemic diseases including T cell tolerance for pollen antigen [21] and vaccination for Japanese encephalitis [17], cancer [18], and human immunodeficiency virus type 1 gp120 [19,20]. Thus, further studies on the safety and efficacy of γ-PGA-Phe NPs as a potent candidate for drug delivery in retinal disorders seem warranted.

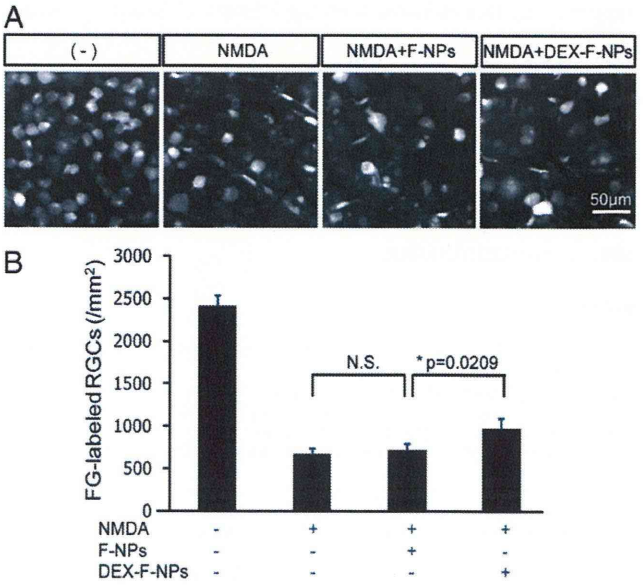

Fig. 12. DEX-F-NPs suppressed NMDA-induced RGC death. A: A representative photograph of FG-labeled RGCs in the flat-mounted retina 7 days after NMDA injection. B: Quantitative data for FG-labeled RGCs. DEX-F-NPs, but not F-NPs, suppressed NMDA-induced RGC death.

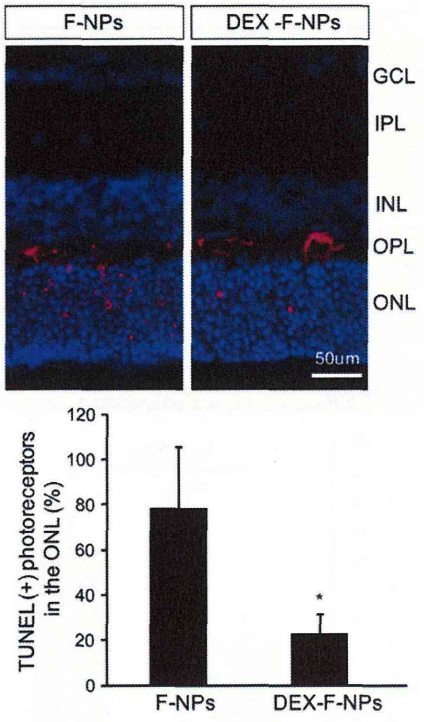

Fig. 13. DEX-NPs suppress retinal detachment-induced photoreceptor degeneration. The upper panels show the TUNEL (+) cells (red signals) and DAPI-nuclear staining (blue signals). The bar charts in the lower panels show the quantitative data from *TUNEL (+) photoreceptors in the ONL and suggest that the DEX-NPs significantly* suppressed the number of TUNEL (+) cells (*: $p = 0.0065$). Scale bar = 50 μm. GCL: ganglion cell layer, IPL: inner plexiform layer, INL: inner nuclear layer, OPL: outer plexiform layer, and ONL: outer nuclear layer.

Acknowledgements

We thank Prof. Larry. I. Benowitz (Children's Hospital, Harvard Medical School) for editing this manuscript and Mr. Jiro Watanabe and Koutaro Yamamoto for technical assistance. This study was supported by Grants-in-Aid from the Ministry of Education, Science and Technology of Japan (21659395 and 22689045, T.N.), the Uehara Memorial Research Foundation, the Takeda Research Foundation, the Imai Glaucoma Research Foundation (T.N.), and CREST from the Japan Science and Technology Agency (T. A. and M. A.).

Appendix A. Supplementary data

Supplementary data to this article can be found online at doi:10.1016/j.jconrel.2010.11.029.

References

[1] D. Ghate, H.F. Edelhauser, Ocular drug delivery, Expert Opin. Drug Deliv. 3 (2) (2006) 275–287.
[2] R. Gurny, T. Boye, H. Ibrahim, Ocular therapy with nanoparticulate systems for controlled drug delivery, J. Control. Release 2 (1985) 353–361.
[3] J.A. Champion, Y.K. Katare, S. Mitragotri, Particle shape: a new design parameter for micro- and nanoscale drug delivery carriers, J. Control. Release 121 (1–2) (2007) 3–9.
[4] U.B. Kompella, N. Bandi, S.P. Ayalasomayajula, Subconjunctival nano- and microparticles sustain retinal delivery of budesonide, a corticosteroid capable of inhibiting VEGF expression, Investig. Ophthalmol. Vis. Sci. 44 (3) (2003) 1192–1201.
[5] H. Kranz, N. Ubrich, P. Maincent, R. Bodmeier, Physicomechanical properties of biodegradable poly(D, L-lactide) and poly(D, L-lactide-co-glycolide) films in the dry and wet states, J. Pharm. Sci. 89 (12) (2000) 1558–1566.
[6] C.X. Song, V. Labhasetwar, H. Murphy, X. Qu, W.R. Humphrey, R.J. Shebuski, R.J. Levy, Formulation and characterization of biodegradable nanoparticles for intravascular local drug delivery, J. Control. Release 43 (2–3) (1997) 197–212.
[7] H.M. Redhead, S.S. Davis, L. Illum, Drug delivery in poly (lactide-co-glycolide) nanoparticles surface modified with poloxamer 407 and poloxamine 908: in vitro characterisation and in vivo evaluation, J. Control. Release 70 (3) (2001) 353–363.
[8] J.H. Kim, K.W. Kim, M.H. Kim, Y.S. Yu, Intravenously administered gold nanoparticles pass through the blood-retinal barrier depending on the particle size, and induce no retinal toxicity, Nanotechnology 20 (50) (2009) 505101.
[9] K. Okabe, H. Kimura, J. Okabe, A. Kato, N. Kunou, Y. Ogura, Intraocular tissue distribution of betamethasone after intrascleral administration using a non-biodegradable sustained drug delivery device, Investig. Ophthalmol. Vis. Sci. 44 (6) (2003) 2702–2707.
[10] N. Kunou, Y. Ogura, M. Hashizoe, Y. Honda, S.H. Hyon, Y. Ikada, Controlled intraocular delivery of ganciclovir with use of biodegradable scleral implant in rabbits, J. Control. Release 37 (1–2) (1995) 143–150.
[11] E. Eljarrat-Binstock, A.J. Domb, Iontophoresis: a non-invasive ocular drug delivery, J. Control. Release 110 (3) (2006) 479–489.
[12] E. Eljarrat-Binstock, F. Raiskup, J. Frucht-Pery, A.J. Domb, Transcorneal and transscleral iontophoresis of dexamethasone phosphate using drug loaded hydrogel, J. Control. Release 106 (3) (2005) 386–390.
[13] G. Zhang, X. Feng, K. Wabner, C. Fandrey, A. Naqwi, T. Wiedmann, T.W. Olsen, Intraocular nanoparticle drug delivery: a pilot study using an aerosol during pars plana vitrectomy, Investig. Ophthalmol. Vis. Sci. 48 (11) (2007) 5243–5249.
[14] T. Akagi, M. Higashi, T. Kaneko, T. Kida, M. Akashi, Hydrolytic and enzymatic degradation of nanoparticles based on amphiphilic poly(gamma-glutamic acid)-graft-L-phenylalanine copolymers, Biomacromolecules 7 (1) (2006) 297–303.
[15] T. Akagi, X. Wang, T. Uto, M. Baba, M. Akashi, Protein direct delivery to dendritic cells using nanoparticles based on amphiphilic poly(amino acid) derivatives, Biomaterials 28 (23) (2007) 3427–3436.
[16] I.L. Shih, Y.T. Van, The production of poly-(gamma-glutamic acid) from microorganisms and its various applications, Bioresour. Technol. 79 (3) (2001) 207–225.
[17] S. Okamoto, H. Yoshii, T. Ishikawa, T. Akagi, M. Akashi, M. Takahashi, K. Yamanishi, Y. Mori, Single dose of inactivated Japanese encephalitis vaccine with poly (gamma-glutamic acid) nanoparticles provides effective protection from Japanese encephalitis virus, Vaccine 26 (5) (2008) 589–594.
[18] T. Yoshikawa, N. Okada, A. Oda, K. Matsuo, H. Kayamuro, Y. Ishii, T. Yoshinaga, T. Akagi, M. Akashi, S. Nakagawa, Nanoparticles built by self-assembly of amphiphilic gamma-PGA can deliver antigens to antigen-presenting cells with high efficiency: a new tumor-vaccine carrier for eliciting effector T cells, Vaccine 26 (10) (2008) 1303–1313.
[19] X. Wang, T. Uto, T. Akagi, M. Akashi, M. Baba, Induction of potent CD8+ T-cell responses by novel biodegradable nanoparticles carrying human immunodeficiency virus type 1 gp120, J. Virol. 81 (18) (2007) 10009–10016.
[20] X. Wang, T. Uto, T. Akagi, M. Akashi, M. Baba, Poly(gamma-glutamic acid) nanoparticles as an efficient antigen delivery and adjuvant system: potential for an AIDS vaccine, J. Med. Virol. 80 (1) (2008) 11–19.
[21] T. Yoshitomi, K. Hirahara, J. Kawaguchi, N. Serizawa, Y. Taniguchi, S. Saito, M. Sakaguchi, S. Inouye, A. Shiraishi, Three T-cell determinants of Cry j 1 and Cry j 2, the major Japanese cedar pollen antigens, retain their immunogenicity and tolerogenicity in a linked peptide, Immunology 107 (4) (2002) 517–522.
[22] T. Nakazawa, T. Hisatomi, C. Nakazawa, K. Noda, K. Maruyama, H. She, A. Matsubara, S. Miyahara, S. Nakao, Y. Yin, L. Benowitz, A. Hafezi-Moghadam, J.W. Miller, Monocyte chemoattractant protein 1 mediates retinal detachment-induced photoreceptor apoptosis, Proc. Natl Acad. Sci. USA 104 (7) (2007) 2425–2430.
[23] T. Nakazawa, A. Matsubara, K. Noda, T. Hisatomi, H. She, D. Skondra, S. Miyahara, L. Sobrin, K.L. Thomas, D.F. Chen, C.L. Grosskreutz, A. Hafezi-Moghadam, J.W. Miller, Characterization of cytokine responses to retinal detachment in rats, Mol. Vis. 12 (2006) 867–878.
[24] T. Hisatomi, T. Sakamoto, K.H. Sonoda, C. Tsutsumi, H. Qiao, H. Enaida, I. Yamanaka, T. Kubota, T. Ishibashi, S. Kura, S.A. Susin, G. Kroemer, Clearance of apoptotic photoreceptors: elimination of apoptotic debris into the subretinal space and macrophage-mediated phagocytosis via phosphatidylserine receptor and integrin alphavbeta3, Am. J. Pathol. 162 (6) (2003) 1869–1879.
[25] T. Nakazawa, C. Nakazawa, A. Matsubara, K. Noda, T. Hisatomi, H. She, N. Michaud, A. Hafezi-Moghadam, J.W. Miller, L.I. Benowitz, Tumor necrosis factor-alpha mediates oligodendrocyte death and delayed retinal ganglion cell loss in a mouse model of glaucoma, J. Neurosci. 26 (49) (2006) 12633–12641.
[26] T. Nakazawa, H. Takahashi, K. Nishijima, M. Shimura, N. Fuse, M. Tamai, A. Hafezi-Moghadam, K. Nishida, Pitavastatin prevents NMDA-induced retinal ganglion cell death by suppressing leukocyte recruitment, J. Neurochem. 100 (4) (2007) 1018–1031.
[27] K. Noda, S. Miyahara, T. Nakazawa, L. Almulki, S. Nakao, T. Hisatomi, H. She, K.L. Thomas, R.C. Garland, J.W. Miller, E.S. Gragoudas, Y. Kawai, Y. Mashima, A. Hafezi-Moghadam, Inhibition of vascular adhesion protein-1 suppresses endotoxin-induced uveitis, Faseb J. 22 (4) (2008) 1094–1103.
[28] T. Akagi, T. Kaneko, T. Kida, M. Akashi, Preparation and characterization of biodegradable nanoparticles based on poly(gamma-glutamic acid) with l-phenylalanine as a protein carrier, J. Control. Release 108 (2–3) (2005) 226–236.
[29] T. Akagi, T. Kaneko, T. Kida, M. Akashi, Multifunctional conjugation of proteins on/into bio-nanoparticles prepared by amphiphilic poly(gamma-glutamic acid), J. Biomater. Sci. Polym. Ed. 17 (8) (2006) 875–892.
[30] T. Yoshikawa, N. Okada, A. Oda, K. Matsuo, Y. Mukai, Y. Yoshioka, T. Akagi, M. Akashi, S. Nakagawa, Development of amphiphilic gamma-PGA-nanoparticle based tumor vaccine: potential of the nanoparticulate cytosolic protein delivery carrier, Biochem. Biophys. Res. Commun. 366 (2) (2008) 408–413.
[31] M. Shimura, T. Nakazawa, K. Yasuda, T. Shiono, T. Iida, T. Sakamoto, K. Nishida, Comparative therapy evaluation of intravitreal bevacizumab and triamcinolone

acetonide on persistent diffuse diabetic macular edema, Am. J. Ophthalmol. 145 (5) (2008) 854–861.
[32] M. Shimura, T. Nakazawa, K. Yasuda, T. Shiono, K. Nishida, Pretreatment of posterior subtenon injection of triamcinolone acetonide has beneficial effects for grid pattern photocoagulation against diffuse diabetic macular oedema, Br. J. Ophthalmol. 91 (4) (2007) 449–454.
[33] J. Baath, A.L. Ells, A. Crichton, A. Kherani, R.G. Williams, Safety profile of intravitreal triamcinolone acetonide, J. Ocul. Pharmacol. Ther. 23 (3) (2007) 304–310.
[34] L.I. Lau, K.C. Chen, F.L. Lee, S.J. Chen, Y.C. Ko, C.J. Liu, W.M. Hsu, Intraocular pressure elevation after intravitreal triamcinolone acetonide injection in a Chinese population, Am. J. Ophthalmol. 146 (4) (2008) 573–578.
[35] M. Shimura, K. Yasuda, T. Nakazawa, T. Shiono, T. Sakamoto, K. Nishida, Drug reflux during posterior subtenon infusion of triamcinolone acetonide in diffuse diabetic macular edema not only brings insufficient reduction but also causes elevation of intraocular pressure, Graefes Arch. Clin. Exp. Ophthalmol. 247 (7) (2009) 907–912.
[36] A. Galor, R. Margolis, O.M. Brasil, V.L. Perez, P.K. Kaiser, J.E. Sears, C.Y. Lowder, S.D. Smith, Adverse events after intravitreal triamcinolone in patients with and without uveitis, Ophthalmology 114 (10) (2007) 1912–1918.
[37] H. Chung, J.J. Hwang, J.Y. Koh, J.G. Kim, Y.H. Yoon, Triamcinolone acetonide-mediated oxidative injury in retinal cell culture: comparison with dexamethasone, Investig. Ophthalmol. Vis. Sci. 48 (12) (2007) 5742–5749.

Tumor Necrosis Factor-α Mediates Photoreceptor Death in a Rodent Model of Retinal Detachment

Toru Nakazawa,[*,1,2] *Maki Kayama,*[2] *Morin Ryu,*[1] *Hiroshi Kunikata,*[1] *Ryou Watanabe,*[1] *Masayuki Yasuda,*[1] *Jiro Kinugawa,*[1] *Demetrios Vavvas,*[2] *and Joan W. Miller*[*,2]

Purpose. Photoreceptor degeneration is a major cause of visual loss in various retinal diseases, including retinal detachment (RD) and neovascular AMD, but the underlying mechanisms remain elusive. In this study, the role of TNFα in RD-induced photoreceptor degeneration was investigated.

Methods. RD was induced by subretinal injection of hyaluronic acid. Photoreceptor degeneration was assessed by counting the number of apoptotic cells with TdT-dUTP terminal nick-end labeling (TUNEL) 3 days after RD and measurement of the outer nuclear layer (ONL) thickness 7 days after RD. As the target of anti-inflammatory treatment, the expression of TNFα, with or without dexamethasone (DEX) was examined in rats by real-time PCR. To understand the role of TNFα in photoreceptor degeneration, RD was induced in mice deficient in TNFα or its receptors (TNFR1, TNFR2, and TNFR1 and -2), or in wild-type (WT) mice by using a functionally blocking antibody to TNFα. $CD11b^+$ cells in the outer plexiform layer (OPL) and subretinal space were counted by immunohistochemistry (IHC).

Results. Treatment with DEX ($P = 0.001$) significantly suppressed RD-induced photoreceptor degeneration and the expression of TNFα. RD-induced photoreceptor degeneration was significantly suppressed with specific blockade of TNFα ($P = 0.032$), in mice deficient for TNFα ($P < 0.001$), TNFR2 ($P = 0.001$), or TNFR1 and -2 ($P < 0.001$). However, lack of TNFR1 did not protect against RD-induced photoreceptor degeneration ($P = 0.060$). Müller cell activation was unchanged in WT and $TNF\alpha^{-/-}$ mice. Recruitment of $CD11b^+$ monocytes was significantly lower in the $TNF\alpha^{-/-}$ mice compared to WT mice ($P = 0.002$).

Conclusions. TNFα plays a critical role in RD-induced photoreceptor degeneration. This pathway may become an important target in the prevention of RD-induced photoreceptor degeneration. (*Invest Ophthalmol Vis Sci.* 2011;52:1384–1391) DOI:10.1167/iovs.10-6509

From the [1]Department of Ophthalmology, Tohoku University Graduate School of Medicine, Sendai, Japan; and the [2]Angiogenesis Laboratory, Massachusetts Eye and Ear Infirmary (MEEI), Department of Ophthalmology, Harvard Medical School, Boston, Massachusetts.

Supported by an Alcon Research Award (JWM), a Bausch & Lomb Vitreoretinal Fellowship (TN), Grants-in-Aid 21659395 and 22689045 from the Ministry of Education, Science, and Technology of Japan (TN), the Uehara Memorial Research Foundation, the Takeda Research Foundation and Imai Glaucoma Research Foundation (TN), and National Eye Institute Grant EY014104 (MEEI Core Grant).

Submitted for publication September 1, 2010; revised October 20, 2010; accepted October 22, 2010.

Disclosure: **T. Nakazawa**, None; **M. Kayama**, None; **M. Ryu**, None; **H. Kunikata**, None; **R. Watanabe**, None; **M. Yasuda**, None; **J. Kinugawa**, None; **D. Vavvas**, None; **J.W. Miller**, None

*Each of the following is a corresponding author: Joan W. Miller, Angiogenesis Laboratory, Massachusetts Eye and Ear Infirmary, Department of Ophthalmology, Harvard Medical School. 243 Charles Street, Boston, MA 02114; joan_miller@meei.harvard.edu.

Toru Nakazawa, Tohoku University Graduate School of Medicine, Department of Ophthalmology, 1-1 Seiryo Aoba-ku Sendai-Shi, Miyagi-ken 980-8574, Sendai, Japan; ntoru@oph.med.tohoku.ac.jp.

Photoreceptors are vulnerable in several retinal disorders, including macular degeneration,[1] retinal detachment (RD),[2–4] diabetic retinopathy,[5] retinopathy of prematurity,[6] and retinitis pigmentosa.[7] In these pathologic conditions, photoreceptors undergo apoptosis.[2,5–7] Therefore, new insights about the mechanisms that underlie photoreceptor degeneration in the ocular diseases would be of clinical interest and could lead to new neuroprotective treatments. Previously, we used the rodent model of RD to clarify the mechanism of RD-induced photoreceptor degeneration. We found that RD-induced photoreceptor apoptosis went through a caspase-dependent[8,9] or caspase-independent pathway.[10] Furthermore, we found that monocytes recruited through the upregulation of monocyte chemoattractant protein (MCP)-1 in Müller glial cells play a neurodestructive role in photoreceptor degeneration.[11,12]

Tumor necrosis factor (TNF)-α is synthesized, mainly in monocytes, as a 26-kDa precursor[13] that is cleaved proteolytically and secreted as a 17-kDa protein.[14] TNFα acts via either the low-affinity TNF receptor (TNFR1) or high-affinity TNF receptor (TNFR2).[15] TNFα is upregulated in several neurodegenerative disorders including multiple sclerosis, Parkinson's disease, and Alzheimer's disease and suppression of TNFα has demonstrated therapeutic effects.[16] In ophthalmic disorders, the vitreous samples from patients with RD contain significantly higher levels of TNFα than samples from patients with other retinal conditions, such as macular hole or idiopathic premacular fibrosis.[17,18] However, the role of RD-induced elevated TNFα on photoreceptor degeneration remains unclear.

Recently, TNFα-suppressing monoclonal antibodies such as infliximab have been successfully used to treat patients with inflammatory ocular disease, including Behçet's disease,[19] diffuse subretinal fibrosis (DSF) syndrome,[20] posterior scleritis,[21] retinal vascular tumors,[22] and neovascular age-related macular degeneration.[23] Thus, if TNFα plays a neurodestructive role in RD-induced photoreceptor degeneration, anti-TNFα treatment may be a good candidate for neuroprotective treatment in retinal diseases. In this study, we induced RD in mice deficient in TNF, TNFR1, and TNFR2 and investigated the role of the TNFα pathway on RD-induced photoreceptor apoptosis.

Materials and Methods

Animals

All animal procedures were performed in accordance with the ARVO Statement for the use of Animals in Ophthalmic and Vision Research and the National Institute of Health Guidance for the Care and Use of

Investigative Ophthalmology & Visual Science, March 2011, Vol. 52, No. 3

Laboratory Animals. The protocol was approved by the Animal Care Committee of the Massachusetts Eye and Ear Infirmary and by the Ethics Committee for Animal Experiments of Tohoku University Graduate School of Medicine.

Adult male Brown-Norway rats, TNFα-deficient mice ($TNF\alpha^{-/-}$), TNF receptor 1 and -2 double-deficient mice ($TNFR^{-/-}$; B6.129SF2J background, 20–25 g; Jackson Laboratory, Bar Harbor, ME), TNFR1-deficient mice ($TNFR1^{-/-}$, C57BL6 background; Jackson Laboratory), TNFR2-deficient mice ($TNFR2^{-/-}$, C57BL6 background; Jackson Laboratory), and age- and sex-matched B6.129SF2J mice or C57BL6 mice (wild-type [WT]) were housed in covered cages. Rats and mice were fed with standard rodent diet ad libitum and kept on a 12-hour light (250 lux)–dark cycle.

Surgical Induction of RD

RD was induced in rats and mice, as previously described.[11,12,24] Briefly, anesthesia was preformed with a mixture of xylazine hydrochloride (mice, 10 mg/kg; rats, 20 mg/kg) and ketamine hydrochloride (100 mg/kg). The pupils were dilated and a sclerotomy was created approximately 1 mm posterior to the limbus with a 30-gauge needle. A Glaser subretinal injector (20-gauge shaft with a 32-gauge tip; BD Biosciences, San Diego, CA) connected to a syringe filled with sodium hyaluronate (HealonGV; Pharmacia and Upjohn Co., Kalamazoo, MI) was then introduced into the vitreous cavity. A retinotomy was created in the peripheral retina with the tip of the subretinal injector, and 2 μL of sodium hyaluronate was slowly injected into the subretinal space (SRS), causing detachment of one half of the retina. One hour before RD, dexamethasone (DEX 1 mg/kg; Sigma-Aldrich, St. Louis, MO) or vehicle was injected intraperitoneally (IP). DEX was first dissolved in 100% ethanol alcohol to 1 mg/mL and then diluted in Dulbecco's phosphated-buffered saline (DPBS) to 0.5 mg/mL. Fifty percent ethanol alcohol in DPBS was used as a vehicle control. To block the TNFα in rat RD, the blocking antibody for TNFα was used (goat anti-rat TNFα, 0.1 μg/μL; R&D Systems, Minneapolis, MN), and goat normal IgG (NGS, 0.1 μg/μL, azide free; R&D Systems) was the control. TNFα blocking antibody 1 μL was injected subretinally RD with a syringe (Hamilton, Reno, NV) equipped with a 32-gauge needle by introducing the tip of needle through the sclerotomy into the SRS and then injecting solution over 3 minutes. RDs were created only in the right eye of each animal, with the left eye serving as the control.

The activities of caspase-8 were measured according to the manufacturer's instruction in a commercially available kit (cat. no. APT171; Millipore, Billerica, MA). The retinal samples (150 μg) were harvested 1 to 3 days after the induction of RD, and these were treated with the vehicle, control IgG (1 μg/mL, 705-035-003; Jackson ImmunoResearch Products, West Grove, PA), and the blocking antibody for TNFα (1 μg/mL, goat IgG, cat. no. AB410-NA; R&D Systems) in mice (8 weeks).

Quantification of TUNEL$^+$ Photoreceptor In Vivo

To assess photoreceptor cell loss and apoptosis quantitatively, we used two methods as previously reported: measurement of the outer nuclear layer (ONL) thickness stained by hematoxylin-eosin (H-E) at 7 days after RD[11] and cell counting with TdT-dUTP terminal nick-end labeling (TUNEL; ApopTag Fluorescein In Situ Apoptosis detection kit S7110; Chemicon International, Inc., Temecula, CA) at 3 days after RD.[11] The number of TUNEL$^+$ cells was counted in a masked fashion. The area of the ONL was measured in the captured images (OpenLab software; Improvision Inc., Lexington, MA), and the cell count per square millimeter calculated.

RNA Extraction and RT-PCR

Total RNA extraction and quantitative RT-PCR was performed as previously reported.[11,12,24] Briefly, total RNA was extracted (RNA Purification System; Invitrogen, Carlsbad, CA) and 3 μm of total RNA was subjected to RT (SuperScript III First-Strand Synthesis System; Invitrogen). First strand cDNAs were amplified using a real-time PCR thermal cycler (ABI7700; Applied Biosystems, Inc. [ABI], Foster City, CA) with a PCR core kit (SYBER Green; Applied Biosystems). The primer sets used in this study were as follows; IL-1β forward- TCAGGAAGGCAGTGTCACTCATTG and reverse- ACACACTAGCAGGTCGTCATCATC; TNF-α forward-CCCAGACCCTCACACTCAGATCAT and reverse- GCAGCCTTGTCCCTTGAAGAGAA; and MCP-1 forward- ATGCAGGTCTCTGTCACGCTTCTG, reverse- GACACCTGCTGCTGGTGATTCTCTT, all of which are described in another publication.[12] For relative comparison of each gene, we analyzed the Ct value of the real-time PCR data with the $^{\Delta\Delta}$Ct method, according to the manufacturer's instructions (ABI). To normalize the amount of sample cDNA added to each reaction, the Ct value of the endogenous control (18rRNA) was subtracted from the Ct value of each target gene.

Adult Mouse Retinal Primary Cultures

Adult primary retinal cultures were prepared as described elsewhere.[11] Briefly, isolated neural retinas were incubated at 37°C for 20 minutes in a CO_2 incubator in a digestion solution containing papain (10 U/mL; Worthington, Lakewood, NJ). Cell density was adjusted to 4.0×10^5 cells each well with neuronal cell growth medium (Neurobasal A, containing B27 supplement, NBA/B27; Invitrogen) and 1 μg/mL insulin, 2 mM L-glutamate, and 12 μg/mL gentamicin. One hour later, TNFα was added to culture medium to reach final concentrations (0.001, 0.01, and 0.1 ng/mL) and cells were incubated for further 24 hours. To assess the viability of photoreceptors, we performed immunocytochemistry (ICC) with rabbit anti-recoverin antibody (1:500 dilution, AB5585; Chemicon), as published.[11] The number of recoverin$^-$ photoreceptors was counted at 10 random fields per well with a fluorescence microscope (×20 objective) equipped with an imaging system, and the number of recoverin$^+$ cells was counted in a blind fashion with ImageJ software (developed by Wayne Rasband, National Institutes of Health, Bethesda, MD; available at http://rsb.info.nih.gov/ij/index.html). Values are given as the mean ± SEM of counts in four replicate wells.

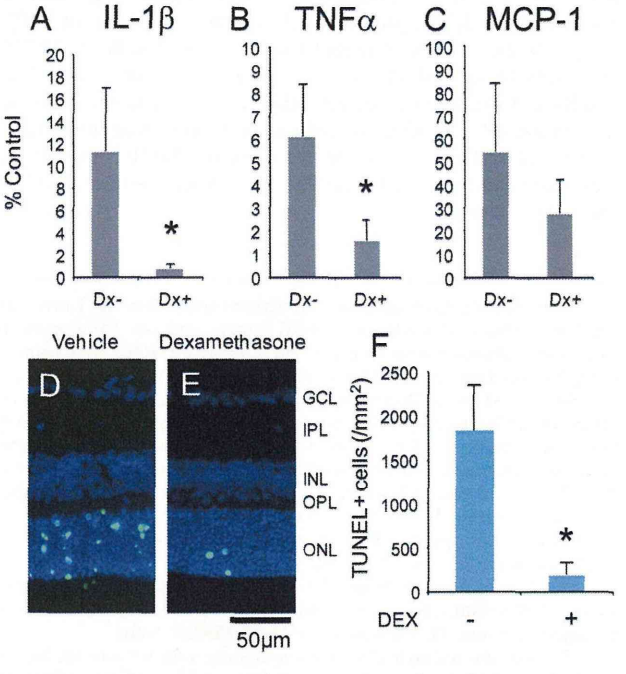

Figure 1. DEX suppresses the expression of cytokines and RD-induced TUNEL$^+$ photoreceptors in rats. (**A–C**) Quantitative real-time PCR data for IL-1β (**A**), TNFα (**B**), and MCP-1 (**C**) mRNA 1 hour after RD ($n = 6$). (**D–E**) Representative photography of detached retina labeled by TNUEL with (**E**) or without (**D**) DEX Quantification of TUNEL$^+$ photoreceptors 72 hours after RD with (+) or without (–) DEX (**F**). *Green*: TUNEL; *blue*: DAPI nuclear staining. $^*P < 0.5$, treated versus untreated condition ($n = 6$ each). GLC, ganglion cell layer; IPL, inner plexiform layer.

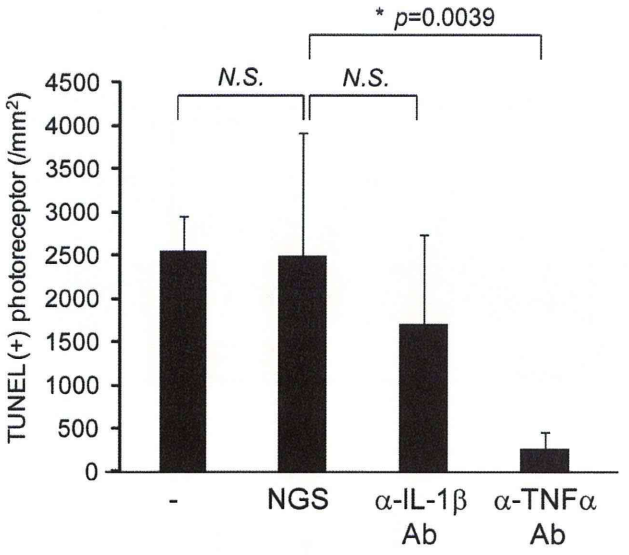

FIGURE 2. A TNFα-blocking antibody prevents RD-induced photoreceptor loss 72 hours after RD in rats. Data are the number of TUNEL$^+$ photoreceptors 72 hours after RD with subretinal administration of α-IL-1β antibody and α-TNFα antibody. NGS, normal goat serum.

Immunohistochemistry

Immunohistochemistry was performed as previously reported.[11,12,24] Briefly, 10-μm retinal sections through the optic nerve head were prepared and subjected to reaction with primary antibodies against phosphorylated ERK (pERK, 1:200; Cell Signaling Technology Inc., Beverly, MA), c-Fos (1:200; Santa Cruz Biotechnology, Inc., Santa Cruz, CA), or CD11b (1:200; Serotec Inc., Raleigh, NC). Retinal sections incubated with a buffer without the primary antibodies were used as negative controls. Fluorescence-conjugated secondary antibodies, including goat anti-mouse immunoglobulin G (IgG) and anti-rabbit IgG and anti-rat IgG conjugated to Alexa Fluor 488 (Molecular Probes, Eugene, OR) were used. Retinal sections were mounted with antifade medium (Vectashield; Vector Laboratories, Burlingame, CA) containing 4′,6 diamidino-2-phenylindole (DAPI) to reveal the nuclear structure. Immunolabeled cells were counted in photomicrographs of the center of the detached retinal area by using a microscope equipped with fluorescence illumination (DMRXA; Leica, Bannockburn, IL) and were analyzed (OpenLab software, ver. 2.2.5; Improvision). The pERK$^+$, c-Fos$^+$, and CD11b$^+$ cells (at ×200 magnification) were counted in a masked fashion.

Statistical Analysis

The statistical significance of the RT-PCR result was determined with the Mann-Whitney U test. The data from the TUNEL and in vitro survival assays were analyzed with the Scheffé post hoc test (StatView 4.11J software for Macintosh; Abacus Concepts, Inc., Berkeley, CA). The significance level was set at $P < 0.05$. The data represent the mean ± SD except for culture results.

RESULTS

Anti-inflammatory Treatment with DEX Suppress the Photoreceptor Death and the Upregulation of TNFα Expression after RD

Previously, we showed that the expression of IL-1β, TNFα, and MCP-1 increased significantly after RD in rats.[12] In the present study, we first investigated the anti-inflammatory effect of the IP-DEX (1 mg/kg) on RD-induced photoreceptor degeneration in rats. This concentration of DEX was chosen because it resulted in a neuroprotective effect on photoreceptors after photodynamic therapy (PDT) in our previous studies.[25] IP-DEX suppressed the RD-induced upregulation of IL-1β expression ($P = 0.004$; Fig. 1A) and TNFα expression ($P = 0.006$; Fig. 1B) 1 hour after RD ($n = 6$), and MCP-1 also showed a trend toward suppression ($P = 0.055$; Fig. 1C). We next investigated whether the IP-DEX anti-inflammatory effect resulted in neuroprotection for the RD-induced photoreceptor degeneration. IP-DEX significantly suppressed the RD-induced photoreceptor degeneration ($n = 9$, $P = 0.0005$; Figs. 1D–F). To examine the role of IL-1β and TNFα on photoreceptor degeneration, we injected anti-IL-1β or anti-TNFα neutralizing antibody subretinally and counted TUNEL$^+$ cells in the ONL 3 days after RD in rats. We found that anti-TNFα antibody significantly decreased the number of TUNEL$^+$ photoreceptors ($P = 0.004$), but anti-IL-1β antibody did not ($P = 0.109$) compared with the effect of normal goat IgG (Fig. 2). These data demonstrate that anti-inflammatory treatment with DEX and anti-TNFα blocking antibody has a significant neuroprotective effect on the RD-induced photoreceptor degeneration.

Cytotoxic Effect of TNFα on Cultured Photoreceptors

To investigate the roles of the increased expression of TNFα after RD, we administered TNFα on cultured photoreceptors

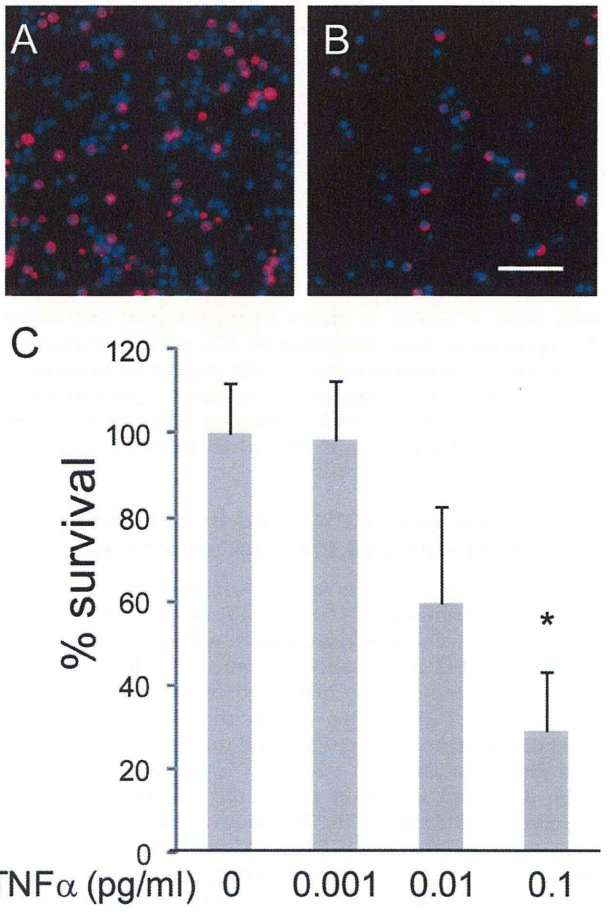

FIGURE 3. Cytotoxicity of TNFα for adult cultivated photoreceptors. (**A**, **B**) Recoverin$^+$ photoreceptors in culture with (**B**) or without (**A**) TNFα. *Red*: recoverin$^+$ photoreceptors; *blue*: DAPI nuclear staining. Scale bar, 100 μm. (**C**) Dose-response effects of TNFα cytotoxicity on recoverin$^+$ photoreceptors. *$P < 0.05$ compared with controls without TNFα.

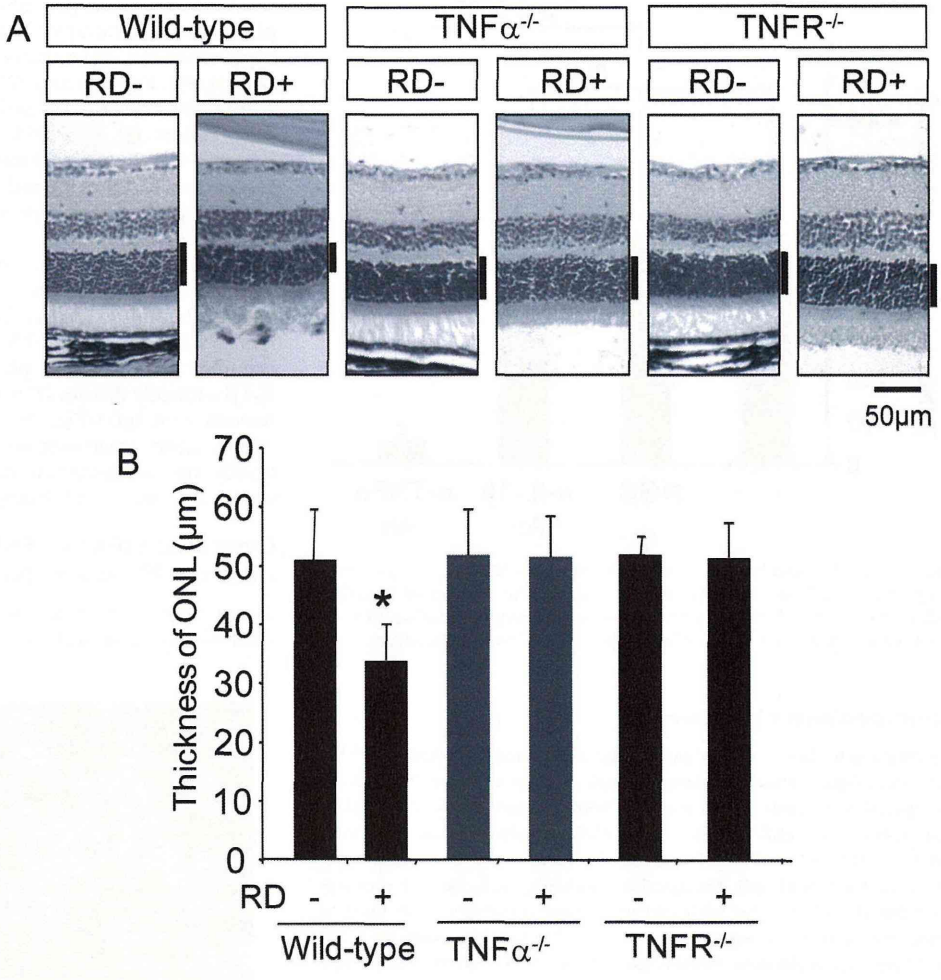

FIGURE 4. Deletion of the *Tnfa* and *Tnfr* genes prevents ONL degeneration after RD in mice. (**A**) H-E-stained sections through the retinas of WT mice, TNFα, TNFR$^{-/-}$, or TNFR1 and -2 with or without RD. (**B**) Quantification of the ONL thick ness with (+) or without (-) RD in WT, TNFα$^{-/-}$, and TNFR$^{-/-}$ mice. *$P <$ 0.05 compared with WT controls without RD ($n = 10$ each).

from adult WT mice in mixed primary retinal cell culture. Photoreceptors were identified by ICC with an antibody to recoverin, a commonly used cellular marker for photoreceptors in vitro.[11] The number of recoverin$^+$ photoreceptors declined progressively with increasing TNFα concentration (Fig. 3), and 0.1 ng/mL of TNFα had significant cytotoxic effects (Fig. 3C).

Genetic Deletion of TNFα and Its Receptor Prevents RD-Induced Photoreceptor Degeneration

TNFα acts via two known receptors, TNFR1 and -2. To investigate the contribution of TNFα and the receptors to the pathophysiological events described earlier, we induced RD in TNFα or TNFR1 and -2 double-knockout mice (TNFR$^{-/-}$). Photoreceptor degeneration was quantified by measuring the ONL thickness[11,24] 7 days after RD. In the absence of RD, the general appearance of the retina and the thickness of the ONL were similar in TNFα $^{-/-}$, TNFR $^{-/-}$, and WT mice (Fig. 4). Seven days after induction of RD, the thickness of the ONL decreased significantly in the WT mice ($P = 0.001$, $n = 10$, Fig. 4). In contrast, after RD in TNFα $^{-/-}$ and TNFR $^{-/-}$ mice, the thickness of the ONL remained unchanged from baseline ($n =$ 10 respectively, Fig. 4). TUNEL at 72 hours after RD showed a greater number of TUNEL$^+$ photoreceptors in the WT mice (2517 ± 210 cells/mm^2) than in the TNFα $^{-/-}$ and TNFR $^{-/-}$ mice ($P < 0.001$); with no TUNEL$^+$ cells in the untreated retinas (Fig. 5). These data suggest that RD-induced upregulation of TNFα has a cytotoxic effect on RD-induced photoreceptor degeneration via its receptors in vivo.

One to 3 days after injury, caspase-8 was significantly active in the detached retina. The blocking antibody for TNFα significantly prevented the activation of caspase-8 (Fig. 6).

RD-Induced Photoreceptor Degeneration Is Mediated Via TNFR2

To further delineate the separate contribution of TNFR1 and -2 to the RD-induced photoreceptor degeneration, we induced RD on TNFR1 or -2 single-knockout mice. In the WT mice, the number of TUNEL$^+$ photoreceptors 72 hours after RD was 2608 ± 262 cells/mm^2 (Fig. 5C) and was similar in the TNFR1$^{-/-}$ mice. In contrast, the number of TUNEL$^+$ photoreceptors in the TNFR2$^{-/-}$ mice was significantly less than that in the WT mice ($P < 0.0001$, Fig. 5C). Thus, RD-induced photoreceptor degeneration appeared to be mediated by TNFα acting via TNFR2.

Effect of TNFα on the RD-Induced Müller Cell Activation

We previously reported that RD activates the intracellular MAPK/c-Fos signaling pathway in the Müller cell immediately after insult and that the response is critical for retinal gliosis and pathogenesis of photoreceptor degeneration.[11,24] The genetic ablation of GFAP and vimentin leads to reduced activation of pERK and c-Fos.[24] To determine whether RD-induced upregulation of TNFα is an upstream event of MAPK/c-Fos activation, we compared the number of pERK$^+$ or c-Fos$^+$ cells in the inner nuclear layer (INL) in the WT mice and TNFα $^{-/-}$

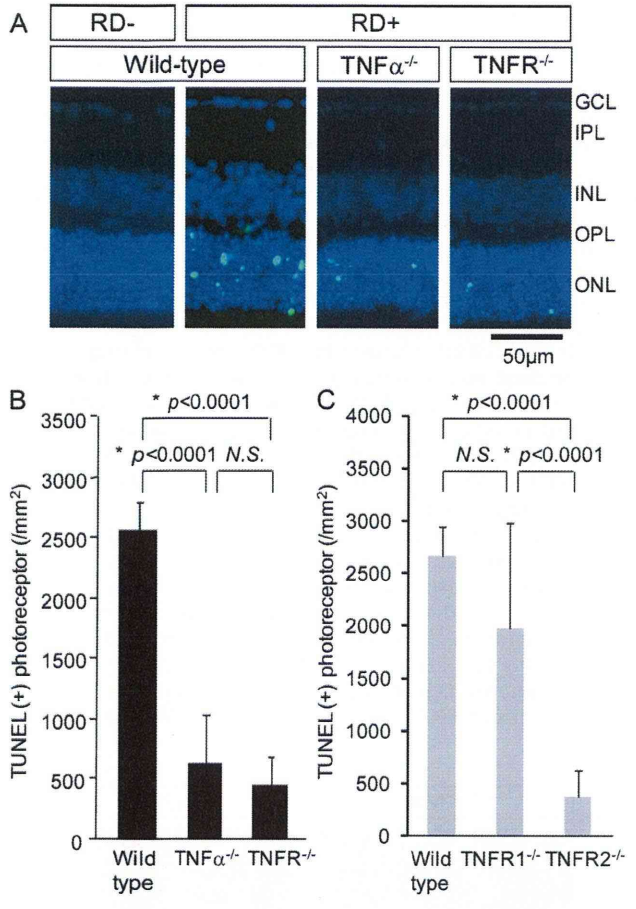

FIGURE 5. Cytotoxic effect of TNFα on RD-induced photoreceptor degeneration. (**A**) Representative photography with TUNEL 72 hours after RD in WT, $TNF\alpha^{-/-}$, and $TNFR^{-/-}$ mice. *Green*: TUNEL; *blue*: DAPI nuclear staining. (**B**) Quantification of $TUNEL^{+}$ cells in WT, $TNF\alpha^{-/-}$, and $TNFR^{-/-}$ mice. $^{*}P < 0.05$ compared with WT mice with RD ($n = 8$ each). (**C**) Quantification of $TUNEL^{+}$ cells in WT, $TNFR1^{-/-}$, and $TNFR2^{-/-}$ mice. $^{*}P < 0.05$ compared with WT mice with RD ($n = 8$ each). GLC, ganglion cell layer; IPL, inner plexiform layer.

mice, before and after RD. Surprisingly, the number of $pERK^{+}$ or c-Fos^{+} cells in the $TNF\alpha^{-/-}$ mice was not significantly different from that in the WT mice (Fig. 7). These data demonstrate that the deletion of TNFα is not related to the retinal glial activation associated with RD.

TNFα Contributes to Monocyte Recruitment in the Detached Retina

We have shown that monocytes recruited after RD mediates their cytotoxic effect on photoreceptors through oxidative stress.[11] To examine the role of TNFα in monocyte recruitment, we investigated whether deletion of the TNFα gene would alter monocyte recruitment after RD. After RD in WT mice, monocytes were recruited to the outer plexiform layer (OPL) and the SRS (Fig. 8). This recruitment was strongly suppressed in TNFα-deficient mice and these data suggest that TNFα plays a critical role in recruiting monocytes to the OPL and SRS after RD.

Discussion

The increased expression of TNFα in the human vitreous in several retinal disorders suggests that TNFα contributes to the pathophysiology of these diseases[17,18]; however, under certain conditions, TNFα plays not only a cytotoxic role but also a neuroprotective one in damaged retinal neurons. Using a mouse model of RD, we showed for the first time that TNFα is a critical mediator of RD-induced photoreceptor death. Acute blockade of TNFα with a functionally blocking antibody or deletion of TNFα or its receptor gene in genetically altered mice almost completely eliminated RD-induced photoreceptor degeneration. We further showed that the cytotoxic effect of TNFα on photoreceptors is mediated through TNFR2 but not -1. These data suggest that anti-TNFα treatment has potential as a neuroprotective therapy for photoreceptor degeneration.

We have previously demonstrated increased expression of IL-1β, TNFα, and MCP-1 in detached retina 1 hour after RD.[12] MCP-1 had a cytotoxic effect on RD-induced photoreceptor degeneration through recruited monocytes,[11] but the roles of IL-1β and TNFα remained unclear. To further explore the role of these cytokines, we administered DEX as an anti-inflammatory treatment to examine its effect on RD-induced photoreceptor degeneration. Interestingly, DEX significantly suppresses the expression of IL-1β and TNFα and reduced photoreceptor degeneration. Generally, IL-1β and TNFα are multifunctional proinflammatory cytokines with effects dependent on the timing and dosage.[26,27] In this study, only acute blockade of TNFα, but not IL-1β, with specific blocking antibody suppressed the RD-induced photoreceptor degeneration. TNFα also has multifunctional roles in the neuronal homeostasis and neuropathology.[28] Previously, we have shown that the expression of TNFα after RD is biphasic (peaking at 1 and 6 hours after RD)[12] and that the source of TNFα is primarily via recruited monocytes and resident microglia and to a lesser extent retinal neurons of all types.[12] Up to now, TNFα has been shown to be a critical mediator for the cytotoxic roles of neurons in various neurodegenerative diseases, including multiple sclerosis, Parkinson's disease, Alzheimer's disease,[16] and glaucoma.[29] On the other hand, TNFα has a neuroprotective role against neuronal damage[30] including retinal ganglion cell death after axotomy by suppressing the potassium channel via channel phosphorylation.[31] In this model of RD, we demonstrated the cytotoxic roles of TNFα on RD-induced photoreceptor degeneration. These data suggest that anti-TNFα or blockade of TNFα receptors may have beneficial effects in the treatment of ocular diseases associated with RD.

The in vitro cytotoxic effect of TNFα on photoreceptors was detectable at a concentration as low as 0.1 ng/mL (Fig. 3). This cytotoxic concentration of TNFα was very similar to the concentration of TNFα (0.095 ng/mL) in the rodent eye after RD.[12] In the vitreous sample of human eyes with RD, the

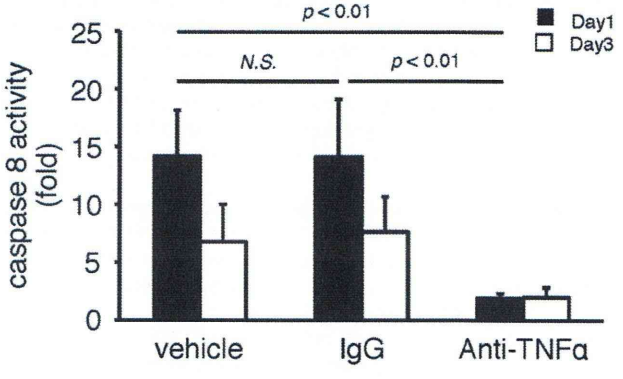

FIGURE 6. Blocking TNFα suppresses RD-induced caspase-8 activation. The data show caspase-8 activation on day 1, declining by day 3 after treatment with anti- TNFα after RD ($n = 4$). NS, not significant.

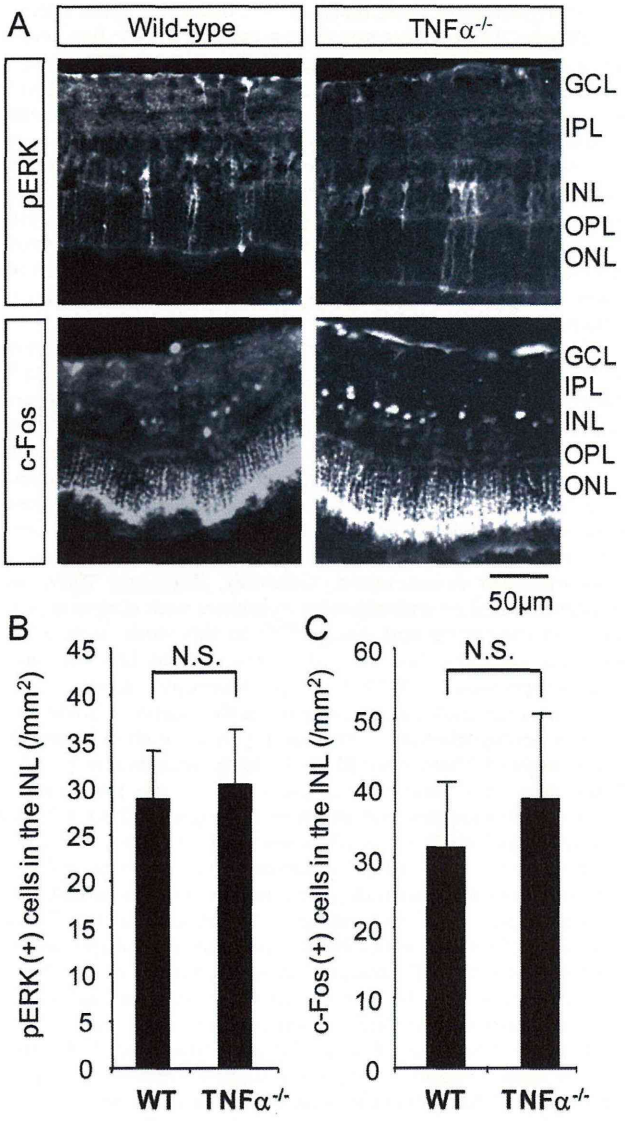

FIGURE 7. Glial activation in the WT mice and TNFα$^{-/-}$ mice in the detached retina. (**A**) Representative photography of IHC with phosphorylated ERK (*top*) and c-Fos (*bottom*) in the WT and TNFα$^{-/-}$ mice. (**B**, **C**) The quantitative data of pERK^{+} (**B**) and c-Fos^{+} (**C**) cells in the INL 72 hours after RD. NS, not significant. GLC, ganglion cell layer; IPL, inner plexiform layer.

concentration of TNFα was reported to be 2 to 22.4 pg/mL[18] and 2.52 to 32.26 pg/mL.[32] In contrast, the subretinal administration of 500 ng/μL of TNFα had no effect on photoreceptor apoptosis 24 hours after RD.[12] Thus, the action of TNFα appears to be influenced by the concentration of TNFα, and the lower concentration (physiological dose) of TNFα results in a neurodestructive effect on RD-induced photoreceptor degeneration.

Our data show that RD-induced photoreceptor degeneration depends on the TNFR2, but not the TNFR1, receptor. Generally, in neurons, TNFR1 has an intracellular death domain and its activation elicits caspase pathways that lead to neuronal cell death. TNFR2, on the other hand, activates the Akt signaling pathway and promotes cell survival.[33] While the role of TNFR2 activation was opposite that in the visual systems, this finding suggests that the role of TNFR2 depends on the tissue. Microglia express both TNFR1 and -2, whereas oligodendrocytes and astrocytes primarily express TNFR1,[34,35] and recruited macrophages express TNFR2.[36] Critical roles of TNFR2 over TNFR1 on the neuronal cell responses had been reported in the axotomized facial motor nucleus through cytotoxic lymphocyte recruitment,[37] and the suppression of oxidative stress in cultivated microglia,[38] as well as the oligodendrocyte regeneration/proliferation and nerve remyelination in demyelinating diseases.[39] We found that RD induced the caspase-8 activation, and the blocking antibody for TNFα suppressed the caspase-8 activation. The data suggest that TNFα activates caspase-8, which is downstream of the TNFα receptor. Thus, the effects of TNFα through its TNF receptors depend on the predominance of the receptor type expression for TNFR1 or -2 in each of the cell types.

This study clearly showed that TNFα activated caspase-8 in the detached mouse retina. On the other hand, there have been some studies in which RD-induced Fas was found to be activated in rats.[40,41] Interestingly, TNFα enhanced the Fas-mediated apoptosis of T cells in the eye.[42] Thus, TNFα may be associated with the FAS pathway in the process of RD-induced photoreceptor degeneration.

The blockade of TNFα had no effect on RD-induced glial activation; however, the recruitment of monocytes was significantly suppressed. We previously reported that recruited monocytes played a critical role in RD-induced photoreceptor degeneration.[11] Moreover, in primary retinal cell cultures, TNFα had a cytotoxic effect on the photoreceptors without macrophage recruitment. Taken together, the neurotoxic roles of TNFα may exert a direct effect on photore-

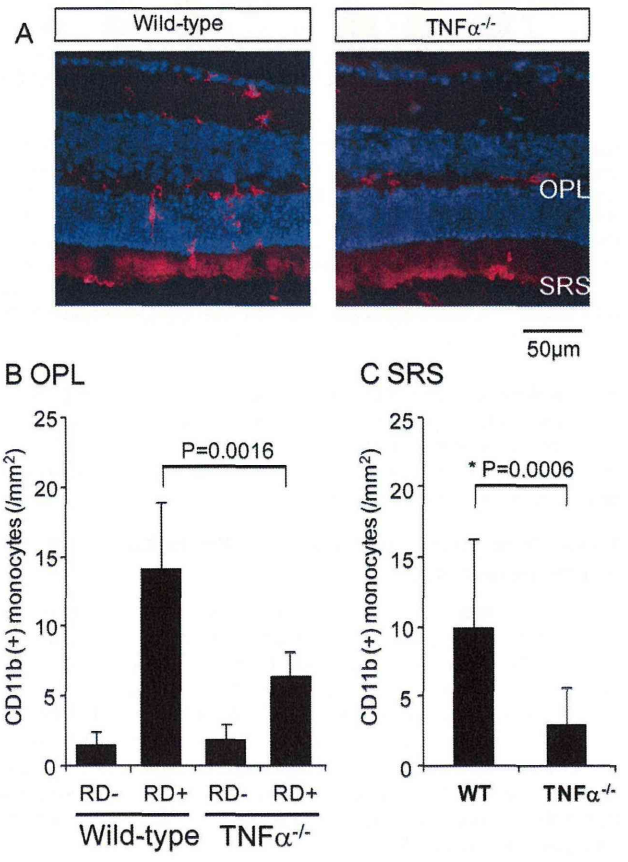

FIGURE 8. Monocyte recruitment is significantly reduced in TNFα$^{-/-}$ mice. (**A**, **B**) Representative photography of IHC with CD 11b (*red*), recruited macrophage and resident microglia in the WT and TNFα$^{-/-}$ mice. (**B**) Data show the number of CD11b^{+} cells in the OPL (**B**) and SRS (**C**) 72 hours after RD in the WT and TNFα$^{-/-}$ mice.